1 2 3	Effects of Improved Simulation of Precipitation on Evapotranspiration and its Partitioning over Land
4 5	Zeyu Cui ^{1†} , Yong Wang ^{1†} , Guang J. Zhang ^{2*} , Mengmiao Yang ³ , Jane Liu ^{3, 4} , and Linyi Wei ¹
6 7	¹ Department of Earth System Science, Ministry of Education Key Laboratory for Earth System Modeling, Institute for Global Change Studies, Tsinghua University, Beijing 100084, China
8	² Scripps Institution of Oceanography, La Jolla, CA, USA
9 10	³ Key Laboratory for Humid Subtropical Eco-Geographical Processes of the Ministry of Education, School of Geographical Sciences, Fujian Normal University, Fuzhou, China
11	⁴ Department of Geography and Planning, University of Toronto, Toronto, Canada
12	
13	
14	
15	
16	
17	Corresponding author: Guang J. Zhang (gzhang@ucsd.edu)
18	†These authors contributed equally to this study.
19	
20	
21	Key Points:
22 23	• The underestimated ratio of transpiration to evapotranspiration can be largely attributed to too frequent light rain.
24 25	• The improved rainfall intensity spectrum greatly impacts evapotranspiration by directly reducing wet leaf fraction and canopy evaporation.
26 27 28	• The associated changes in solar radiation and other factors also affect evapotranspiration by increasing vegetation transpiration.

Abstract

Evapotranspiration (ET) is a key component of the global hydrological cycle, which is strongly modulated by the occurrence of different rainfall intensities. Global climate models (GCMs) commonly suffer from "too much light rain" and a negative bias in the ratio of transpiration (T) to ET (T/ET). It is unclear whether these biases are related. Here we show that with the improved simulation of probability density functions of rainfall intensity by suppressing light-rain occurrence using a stochastic convection parameterization in the NCAR CESM1.2, the canopy T increases in tropical forests while evaporation from canopy interception and bare soil decreases. The simulated T/ET is increased by 2.5% globally and up to 8% regionally, primarily attributable to reduced fraction of wet leaves due to less frequent light rain despite its weak intensity. These results imply that excessive light rain is an important cause of the negative T/ET bias in GCMs.

Plain Language Summary

Water moves from the land surface to the atmosphere via evapotranspiration. Processes contributing to evapotranspiration (ET) include evaporation from soil and wet leaves, and transpiration through pores in plants (T). Rainfall intensity is known to be an important factor in regulating canopy interception and soil moisture, thus impacting ET. "Too much light rain and too little heavy rain" and underestimated ratio of T to ET (T/ET) are two common weaknesses of current global climate models (GCMs). Here we examine the impact of rainfall intensity on climatological ET and show that light rain has a major influence on ET and its components. By improving the representation of convection, the light rain (1-20 mm d⁻¹) frequency is reduced. As a result, the fractional coverage of wet leaves of vegetation decreases, resulting in an increase in T and a decrease in evaporation from canopy interception and bare soil. Therefore, in GCMs, the issue of excessive light rain is a cause of the problem of underestimated T/ET.

1 Introduction

Terrestrial evapotranspiration (ET) is a critical component of the global hydrological cycle and surface energy balance. It also represents a central link with the carbon cycle through plant growth (Wang and Dickinson, 2012; Humphrey et al., 2021; Taylor et al., 2012). ET is governed by near-surface meteorological conditions, plant physiology and structures, and soil moisture status. It is generally recognized that ET over land is limited by available soil moisture when the soil moisture content is low (Teuling et al., 2010), and it responds more to variability in atmospheric conditions such as solar radiation, precipitation, wind speed and relative humidity when there is sufficient soil moisture (De Boeck and Verbeeck, 2011; Costa et al., 2010; Massmann et al., 2019).

Three processes together constitute ET over land, namely plant transpiration (T), evaporation from vegetation canopy (Ec), and evaporation from bare soil (Es). Due to the lack of global-scale observations of ET, let alone its partitioning, large uncertainty exists in quantifying the ratio of T to ET (T/ET) in land surface models (LSMs). In Phase 5 of the Coupled Model Intercomparison Project (CMIP5) simulations, T/ET varies from 0.22 to 0.58 (Wei et al., 2017). Global climate and vegetation models suggest that transpiration is the dominant component at the global scale (Dirmeyer et al., 2006; Jasechko et al., 2013; Good et al., 2015). For example, by constraining the models with 33 field measurements, the most recent estimate of the global average of T/ET from CMIP5 models is 0.62 ± 0.06 (Lian et al., 2018). Thus, an underestimation of T/ET widely exists in global climate models (GCMs).

Among factors influencing ET, rainfall is one of the most important (Laio et al., 2001; Mutti et al., 2019). A CMIP5-based study indicated a positive linear and significant correlation between rainfall bias and ET bias in all models (Li et al., 2018). Using an offline LSM forced by atmospheric reanalysis, for a given rain event, Qian et al. (2006) adjusted rainfall intensity and duration while keeping daily rainfall amount unchanged. They found that rainfall intensity has profound impacts on evaporation and runoff. GCMs have many known biases in the rainfall simulation, one of which is "too much light rain and too little heavy rain" (e.g., Chen et al., 2021). In the meantime, all GCMs underestimate transpiration and its ratio to evapotranspiration. Whether the biases of ET and its associated partitioning are linked to the bias of rainfall intensity spectrum in a coupled land-atmosphere system is unclear. If they are, does it mean that light rain has a disproportionate impact on ET and its partitioning via its high occurrence frequency despite its weak intensity? Besides these, distinct environmental conditions such as clouds, radiation, and surface temperature in different rainfall events impact ET as well. How are they related to ET in different rainfall regimes?

Recently, Wang et al. (2016, 2021) successfully suppressed the excessive occurrence of light rain by incorporating a stochastic convective scheme (Plant and Craig, 2008) into the Zhang-McFarlane deep convection scheme (Zhang and McFarlane, 1995) in two GCMs. The improved rainfall frequency simulation provides a unique opportunity to address the above questions. The paper is organized as follows. Section 2 introduces model experiments and data. The impacts of the improved rainfall frequency spetrum on ET are presented and discussed in section 3. Section 4 examines contributions to ET changes from the broader environmental changes in the simulations. Concluding remarks are given in section 5.

2 Model experiments and data

The GCM used in this study is the NCAR Community Earth System Model version 1.2 (CESM1.2; see supplementary Text S1). The land component of CESM1.2 is the Community Land Model version 4 (CLM4; Oleson et al., 2010). The atmospheric component is the Community Atmosphere Model version 5.3 (CAM5.3; Neale et al., 2010), with a horizontal resolution of 1.9° × 2.5° and a vertical resolution of 30 layers from the surface to 2.26 hPa. Deep convection is parameterized following Zhang and McFarlane (1995; hereafter referred to as ZM scheme) along with dilute convective available potential energy modification (Neale et al., 2008). The stochastic convection scheme of Plant and Craig (2008) is incorporated into the ZM scheme in CAM5.3. A detailed description of the implementation of the stochastic scheme and its overall performance in the climate models can be found in Wang et al. (2016, 2021). Two AMIP-type simulations are conducted using the observed monthly sea surface temperatures and sea ice extent as lower boundary conditions, with the standard ZM scheme (CAM5) and the addition of the stochastic scheme (STOC), respectively. Both simulations are run for 11 years from January 1 1985 to December 31 1995, and the last 10 years are used for analysis.

To evaluate the characteristics of simulated precipitation, the daily Tropical Rainfall Measuring Mission (TRMM) 3B42 version 7 products (Huffman and Bolvin, 2013), the Multi-Source Weighted-Ensemble Precipitation (MSWEP) version 2.8 products (Beck et al., 2019) and the precipitation data from the Global Soil Wetness Project II (GSWP-2; Dirmeyer et al., 2006) are used as benchmarks. To assess evapotranspiration, the FLUXCOM (Jung et al., 2019), the Global Land Evaporation Amsterdam Model (GLEAM) version 3.5 (Martens et al., 2017; Miralles et al., 2011) and the GSWP-2 datasets are used (see details in supplementary Text S2). For a

consistent comparison, the original high-resolution data are regridded to the same latitude-longitude grids as the model.

3 Impacts of rainfall simulation on ET

As precipitation is a major driving force for the land surface hydrological cycle (Oki and Kanae, 2006), its simulation using different convective schemes has a large impact on ET. Rainfall intensity and frequency are two important characteristics of rainfall, and both can regulate ET. Figure 1 shows the global distribution of frequency changes of no-rain, light rain, and moderate-to-heavy rain from CAM5 to STOC, and changes in ET and its three components (T, Ec, and Es). Here no-rain, light rain and moderate-to-heavy rain days are defined as $P < 1 \text{ mm d}^{-1}$, $1 \le P < 20 \text{ mm d}^{-1}$ (Na et al. 2020), and $P \ge 20 \text{ mm d}^{-1}$, respectively. There is a large increase in no-rain frequency over tropical land within 30° S–30° N, by up to 30%. All these increases are entirely at the expense of decrease of light rain frequency, with only a slight increase of moderate-to-heavy rain frequency, by less than 5% except in the Amazon, Congo, and Southeast Asian rainforests. The total amount and the diurnal cycle of rainfall do not change much (Figs. S1-2).

ET is greatly affected by the changes in rainfall frequency and intensity, especially over tropical land. There are clear differences between ET changes in vegetated areas and deserts, with significant increases of ET in vegetated areas of South America, Africa, Australia, and the maritime continent, by up to 150 mm yr⁻¹, but notable decreases in forests along the tropical coastline, such as those in Guyana, the continental margins of West Africa and South Asia. Over desert areas such as the Sahara Desert, the Arabian Desert, the Thar Desert, deserts of Australia, and the Namib Desert, ET are significantly reduced, by up to 150 mm yr⁻¹. Over most vegetated areas, changes in ET are a result of increasing T and Es and decreasing Ec, whereas over desert areas the decrease of ET is mainly from Es.

A tight relationship between changes of Ec and light-rain (or no-rain) frequency is found. Their global distributions are highly correlated, with a correlation coefficient of 0.71 at a 95% significant level. This implies that light rain frequency plays an important role in regulating canopy evaporation. In contrast, there is no similarity of changes between total rainfall amount and Ec. The increase of soil evaporation within the canopy is weakly linked with the increase of the frequency of moderate-to-heavy rain, showing a correlation coefficient of 0.3 in the tropics, while the decreased Es in deserts is strongly related to the light-rain frequency, with a correlation coefficient of 0.8.

Based on results from Fig. 1, the estimated globally averaged ratio of T/ET is increased from 51.8% to 54.3% and the tropical average T/ET is increased from 57.6% to 60.7%, mainly due to reduced Ec and enhanced T over tropical woodlands, where T/ET increases by as much as 8%. This suggests that the overstimulated light rain frequency partly contributes to the negative T/ET biases in GCMs.

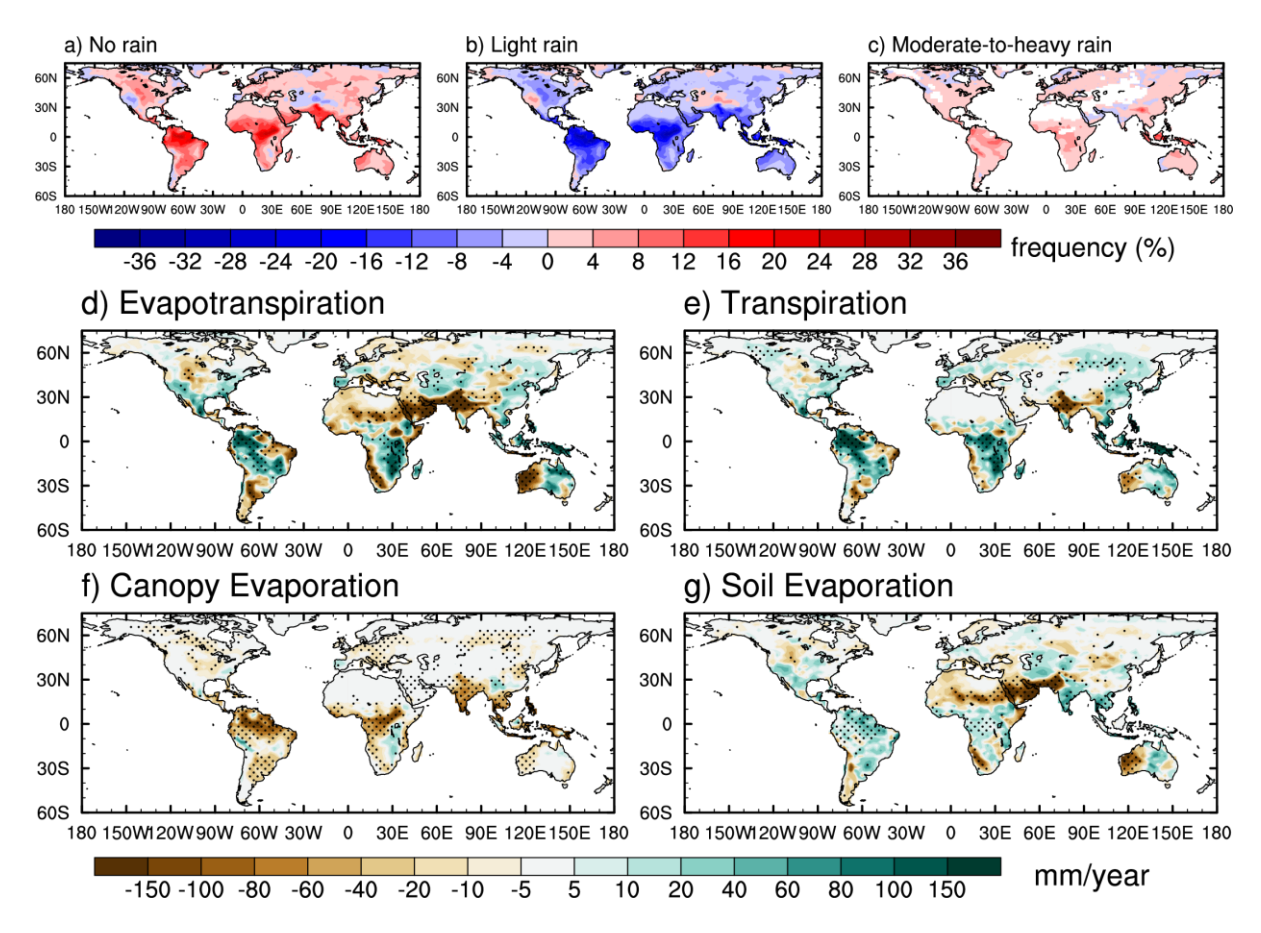


Figure 1. Global distributions of annual differences in frequency (% of days) of (a) no rain (P < 1 mm d⁻¹), (b) light rain ($1 \le P < 20$ mm d⁻¹) and (c) moderate-to-heavy rain ($P \ge 20$ mm d⁻¹), and differences (mm yr⁻¹) in (d) evapotranspiration, (e) transpiration, (f) canopy evaporation, (g) soil evaporation between the CAM5 and STOC simulations (STOC minus CAM5). The latitude range is 60°S-75°N. In (d-g), the differences statistically significant at 95% confidence level are stippled.

The simulated rainfall intensity probability density functions (pdfs) are shown in Figure 2. Only grid points over tropical land (30° S–30° N) are sampled, where the rainfall frequency varies the most. Both observations and simulations show a nearly exponential decrease of frequency of occurrence with rainfall intensity. The pdf in STOC is very close to that from TRMM observations and is within the uncertainties among different observational datasets. The frequency of light-rain events is greatly reduced while the frequency of moderate-to-heavy events is increased.

The correlation between ET (or its components) and concurrent rainfall as well as within ±5 days are calculated (Fig. S3). Although rainfall in prior days can affect ET on the current day, and vice versa, the lead-lag correlation shows that ET and its components have the highest correlation with concurrent rainfall over most of the tropical areas, especially in vegetated areas. Therefore, the following analysis focuses on variations in ET components conditionally sampled on concurrent rainfall events. All daily data including both wet and dry days are divided into bins with an equal bin interval of 0.5 mm d⁻¹. The sum of ET within each bin is then divided by the sum of ET over all bins to obtain the fractional contribution from each bin (Text S3.1). In both observations and simulations, the distribution of ET contribution from different rainfall intensities, including no-rain, to the total ET generally resembles the frequency distribution of rainfall

176

177

178

179

180

181

182

183

184 185

186

187

188

189

190

191

192

193 194

195

intensity (Figs. 2a&b). Since contributions from each bin is the product of the occurrence frequency and the corresponding bin-averaged ET (Text S3.1), the approximately linearly varying or constant bin-averaged ET for different rainfall intensities (Fig. S4) compared to the exponential decrease by several orders of magnitude of occurrence frequency shows the dominant role of rainfall frequency in affecting ET and its components. The pdfs of ET from TRMM/FLUXCOM and MSWEP/GLEAM pairs are very close to each other while the GSWP-2 data has lower ET contributions from rain rates > 20 mm d⁻¹. CAM5 systematically underestimates ET contributions from rain rates > 20 mm d⁻¹ and overestimates them from lower rain rate regimes. The pdf of ET contribution from STOC falls in between those from TRMM/FLUXCOM and MSWEP/GLEAM, indicating its close agreement with observation-based products. Figs. 2c-e show the comparison of model simulations with MSWEP/GLEAM and GSWP-2 for T, Ec and Es. CAM5 again overestimates the fractional contribution of T (or Ec and Es) under light rain and seriously underestimates the contribution of T (or Ec and Es) under heavy rain. The STOC simulation shows a close agreement with the observations for the contribution of ET components, although somewhat underestimates (overestimates) that of Ec and Es and considerably overestimates (underestimates) that of T from light (moderate-to-heavy) rain. The cumulative contributions from rain rates < 20 mm d⁻¹ also show better agreement between STOC and observations for ET and its components, except for Ec, which is underestimated due to underestimation from rain rates less than 6 mm d⁻¹ (Fig. 2 inset). In addition, they show that over 95% or more of ET and its components come from contributions of no-rain and light-rain days except Ec for which moderate-to-heavy rain events have more contribution.

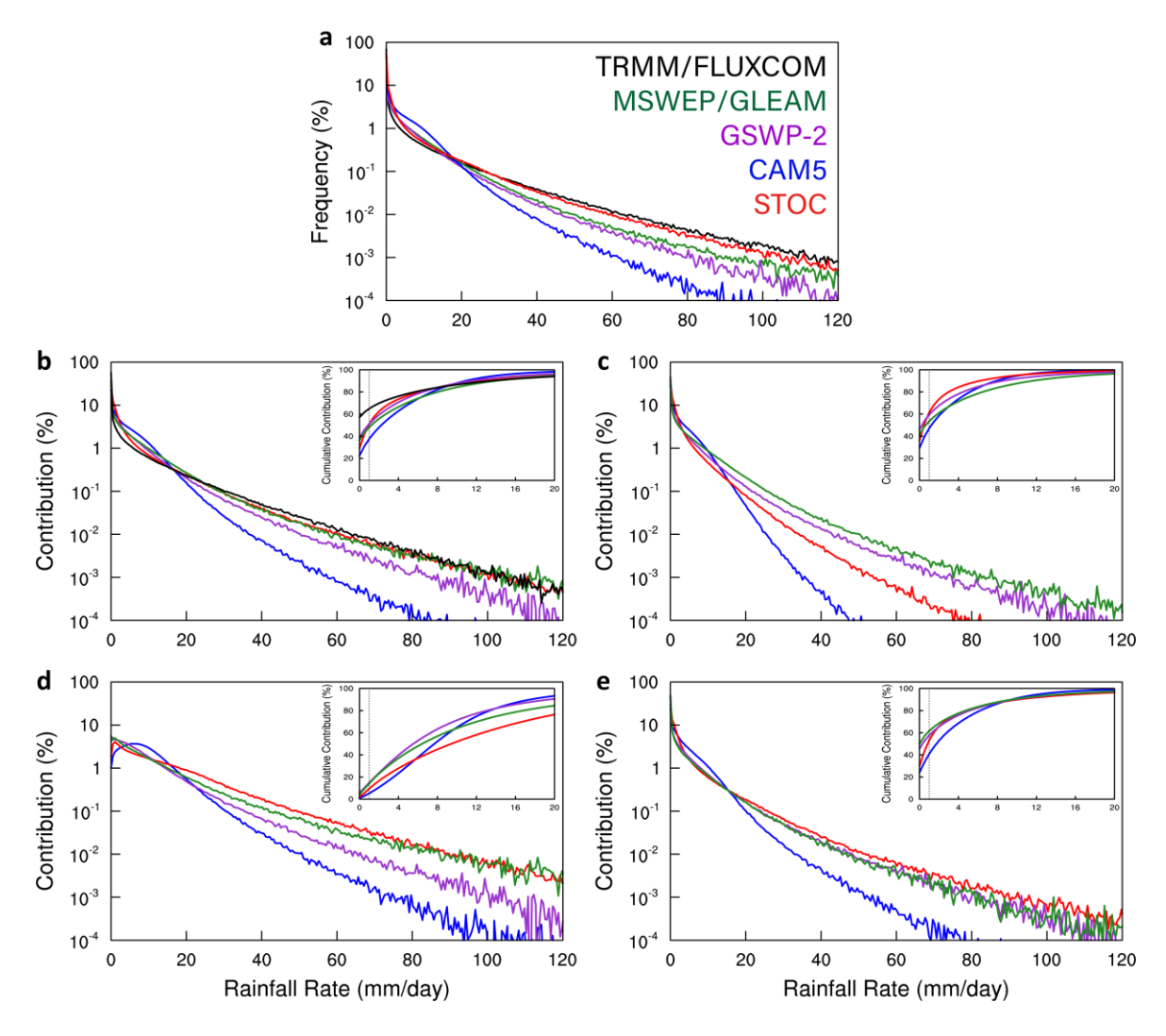


Figure 2. (a) Frequency distributions of rainfall intensity over tropical (30° S–30° N) land from TRMM, MSWEP, GSWP-2, CAM5 and STOC simulations. (b) Fractional contributions of ET under different rainfall intensities to the total ET over tropical (30°S–30°N) land from FLUXCOM, GLEAM, GSWP-2, CAM5 and STOC simulations. (c-e) The same as (b), but for (c) T, (d) Ec, and (e) Es. Bin intervals of 0.5 mm d⁻¹ are used for rainfall rates. The inset frames at the upper right corner are zoomed to the cumulative contributions from rain rates between 0 to 20 mm d⁻¹. The dashed line marks the rain rate of 1 mm d⁻¹, delimiter between no-rain and light rain.

As T occurs on dry leaves of vegetation only and Ec takes place on wet leaves only (Oleson et al., 2004), Figure 3a-d shows changes of T/ET, T, Ec and fraction of wet leaves (Fwet) as functions of light rain changes for different simulated leaf area indices (LAI; Fig S1b). The percentage changes in T and its ratio (T/ET) are negatively correlated with percentage changes in light-rain frequency, and the slope of the linear fit becomes steeper as LAI increases. The areas with LAI<1, where the ET mostly comes from soil evaporation, are excluded. Different from T and T/ET, the percentage changes in Ec and Fwet are positively correlated with changes in the light-rain frequency. The slope of the linear fit also increases with LAI. This is because a higher portion of water could be potentially intercepted from each rainfall event for denser vegetation (Gash et al., 1980; Miralles et al., 2010). In CLM4, the percentage of rainfall intercepted is

proportional to the product of total rainfall and plant density (Oleson et al. 2004). Because of its frequent occurrence, light rain strongly regulates ET and its partitioning over densely vegetated areas despite its weak intensity. Figure 3e shows the changes of ET and its components from CAM5 to STOC as functions of LAI. The ET change is negative in areas with LAI<1, increasing gradually to become positive for LAI>5. The Ec changes are negative for all LAI values and the magnitude increases with LAI. The T changes are mostly insignificant for LAI<5 but strongly positive for LAI>6, largely offsetting the Ec changes. The Es changes are negative for LAI<1, and small positive for LAI>2. Clearly, the ET changes are dominated by different components dependent on the LAI.

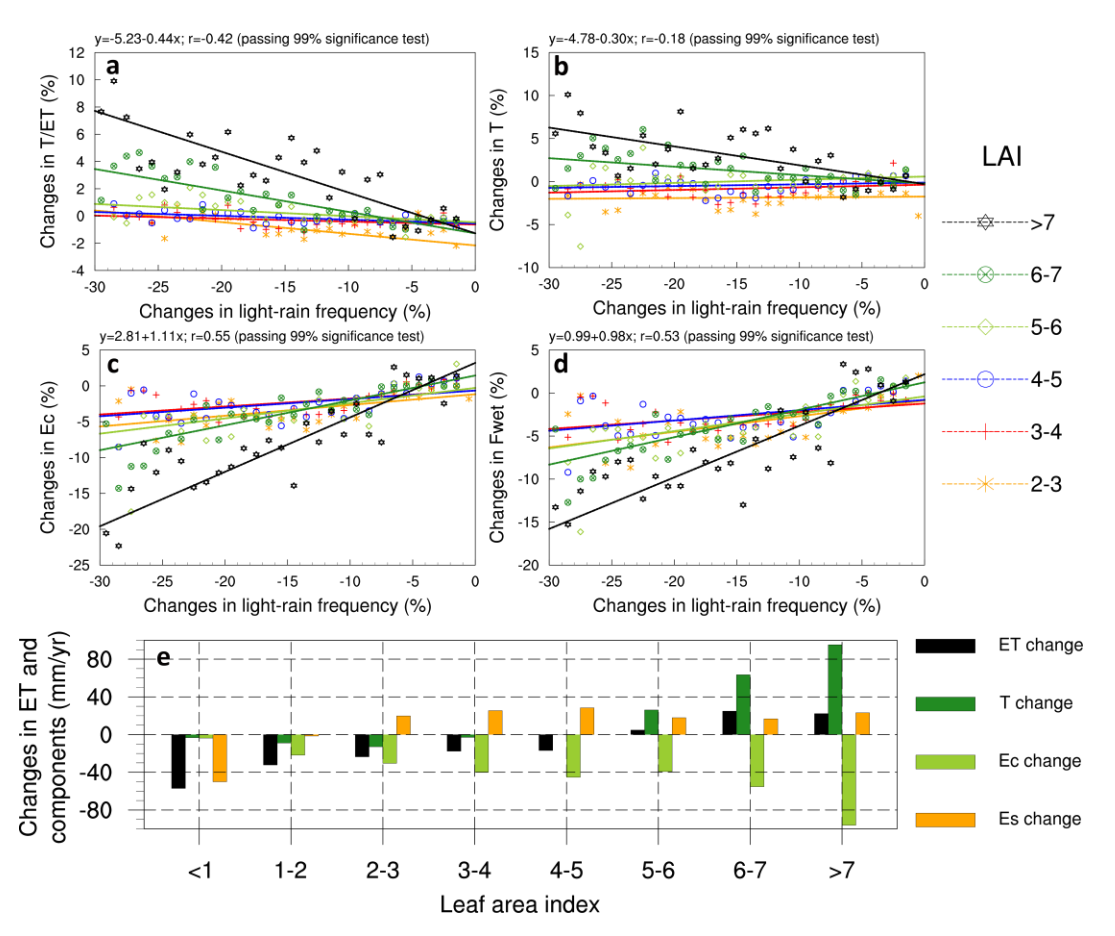


Figure 3. (a-d) Scatter plot of bin-averaged percentage change (%) in the light rain frequency versus percentage change in (a) the ratio of T/ET, (b) T, (c) Ec and (d) fraction of wet leaves (Fwet). (e) Box chart of average amount of changes (mm yr⁻¹) in ET, T, Ec and Es in areas with varying degrees of vegetation over tropical land (30° S–30° N). The changes are calculated from differences between CAM5 and STOC simulations. In (a-d), different colored dots represent grid points with different LAI and the colored lines are the best fit between the two variables. The

equation for the linear relationship between the two in regions with LAI ≥ 2 and the correlation coefficient r are given above each frame.

4 Impacts of environmental changes on ET

230

231

232

233

234

235236

237

238

239

240

241

242

243

244

245

246

247

248

249

250

251

252

253

254

255

256

Qian et al. (2006) also found that rainfall frequency and intensity have large impacts on ET when running the NCAR CLM offline driven by reanalysis data. However, factors that are also important to evapotranspiration, such as solar radiation, surface air temperature and humidity etc., were not considered. In this study, by modifying the convection scheme, the clouds, radiation, atmospheric temperature, moisture, and circulation are all affected (Wang and Zhang, 2016). As such, the environmental conditions are different in CAM5 and STOC. Here we further examine their roles in regulating ET and its components.

Figure 4 shows the spatial distribution of changes in four factors: Fwet, incident solar radiation, vapor pressure deficit (VPD, defined as the difference between the near-surface saturated water vapor pressure and the actual water vapor pressure) and soil moisture, and the dominant factor contributing to the ET changes. Among these factors, Fwet is more directly associated with rainfall characteristics than the rest. The wet leaves decrease by 10%-15% in rainforests in Amazon, Congo, and Indonesia. As expected, the global pattern of the wet leaf decrease highly resembles the pattern of decrease in light rain, indicating that light rain plays a dominant role in wetting leaves due to its frequent occurrence. Closely related to the decrease of light rain and increase of no-rain days, there is more solar radiation reaching the plant canopy and bare soil (Fig. 4b). Accordingly, the near-surface atmosphere is warmer and drier, leading to increased VPD (Fig. 4c). Light rain is effective in moistening soil with little runoff (Trenberth et al., 2003). Therefore, the spatial pattern of changes in soil moisture is similar to changes in light rain (Fig. 4d). Overall, due to the decrease in light rain frequency and increase in no-rain frequency, both the wetness of vegetation canopy and the atmospheric/soil conditions undergo significant changes. We also performed a cursory examination of surface runoff, an important parameter in land surface hydrological cycle, and found that its changes are mostly related to annual-mean total precipitation.

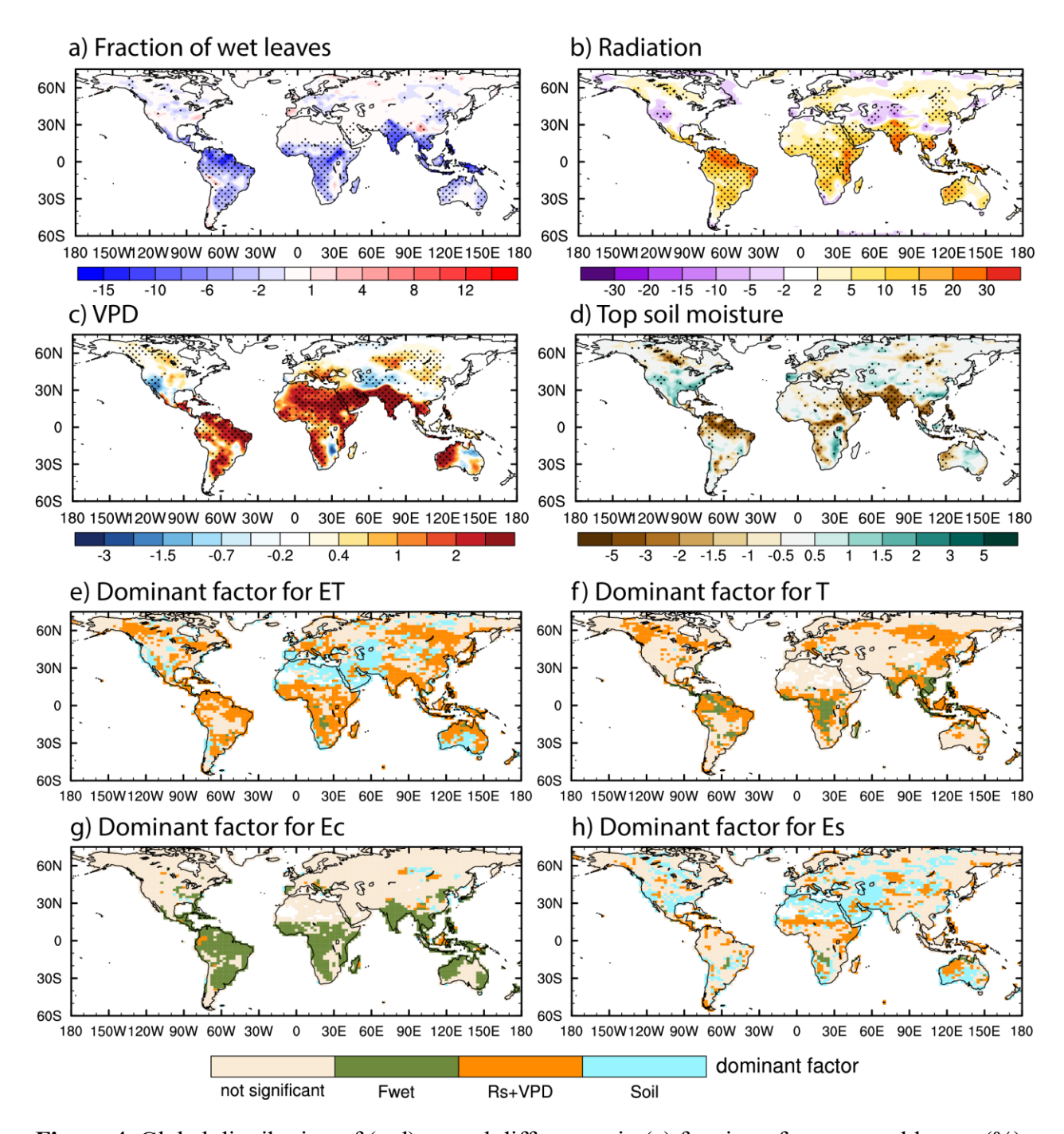


Figure 4. Global distribution of (a-d) annual differences in (a) fraction of wet to total leaves (%), (b) downward shortwave radiation at the surface (W m⁻²), (c) vapor pressure deficit (VPD; hPa) and (d) top soil moisture (defined as soil moisture from the surface to 10 cm; kg m⁻²) between the CAM5 and STOC simulations (STOC minus CAM5), and (e-h) the dominant factor over land for changes in (e) ET, (f) T, (g) Ec, and (h) Es, based on the stepwise MLR analysis. In (e-h), only results significant at 95% confidence level are shown by colors. The regions shown as "not significant" mean that changes caused by all factors are less than the unexplained term in the regression equation or less than 5 mm yr⁻¹, "Fwet" means the dominance of Fwet, "Rs+VPD" atmospheric influence, which combines solar radiation and VPD, and "Soil" soil moisture.

Figure 4 also shows the geographical distribution of the major influencing factor for the changes in ET, T, Ec and Es, respectively. We perform a stepwise multiple linear regression (MLR, Jung et al. 2017; Peng et al. 2013) analysis to identify the major influencing factor among the vegetation (Fwet), atmospheric (radiation and VPD) and soil (topsoil moisture) conditions, using 10-year daily output of the two simulations (Text S3.2). The changes in the four influencing factors together can well explain the changes in ET (with an explained variance of 77%; Fig. S5a), T (82%; Fig. S5b) and Ec (72%; Fig. S5c) over the tropical woodland and the changes in Es (62%; Fig. S5d) over the tropical desert.

Note that VPD usually increases with radiation, thus we combine them into a single factor in Figs. 4e-h. In most land areas with sufficient water, the total ET is mainly regulated by atmospheric conditions, while in deserts soil moisture is a more important constraining factor. In terms of the components of ET, T in the tropics is affected by both atmospheric conditions and biophysical properties (Fig. 4f). Solar radiation and VPD affect transpiration by modulating available energy, driving force, and stomatal regulation of plants. Generally, radiation can enhance T by increasing both available energy and stomatal conductance. However, an increase in VPD can impact T positively by enhancing the driving force but negatively by reducing stomatal conductance. Here T is enhanced by more radiation and suppressed by the correspondingly increased VPD (Fig. S6). T is negatively correlated to the fraction of wet leaves. When leaves are wet, usually after rain, the relative humidity near leaves is close to 100% and the driving force is close to zero. Therefore, T is inhibited. Overall, T is more influenced by atmospheric factors in the tropics. But changes in the fraction of wet leaves seem crucial in several tropical woodlands (e.g., forests around the State of Amazonas in Brazil, Congo rainforest, forests in southern India and the Indochina Peninsula), where T shows a substantial increase (Fig. 1). Soil moisture is not a limiting factor in tropical woodland due to the abundance of soil moisture there.

The relationship between Ec and wet leaves is dominant almost in all tropical vegetated land (Fig. 4g). The similar patterns of the decreases in light rain frequency, the fraction of wet leaves, and Ec illustrate the role of light rain in regulating canopy interception and evaporation. As the excessively high frequency of light rain in CAM5 is suppressed and the frequency of no rain is increased, canopy interception is reduced, and so is Ec. The dominant factor is different for soil evaporation (Fig. 4h). No environmental factors dominate the changes in Es in most of the vegetated lands, whereas soil moisture is the main limiting factor for Es in most desert regions.

5 Concluding remarks

Rainfall frequency and intensity can greatly impact the land-atmosphere interaction through evapotranspiration. This study investigates the implication of the improved rainfall simulation on ET and its partitioning. The results show that the change of rainfall intensity spectrum has profound impacts on ET (Fig. 1). ET increases significantly in forest areas and decreases systematically over deserts, with the magnitude of changes as large as 150 mm yr⁻¹. In savannas and deserts over southeast South America, southeast and north Africa, ET changes are partly due to increases of total rainfall, whereas in tropical rainforests, ET changes result from changes in rainfall intensity spectrum.

By separating contributions of ET in different rainfall intensities to the total ET, we find that light rain has a large effect on ET, whether for transpiration or evaporation of canopy and soil (Figs. 2&3). This is due to its frequent occurrence despite its weak intensity. With an excessively high frequency of light rain compared with observations, the portion of the overall ET in the default

model during light rain periods is overestimated. Moreover, the overstimulated light rain could be 311 an important cause of the negative T/ET biases common in GCMs. Because of suppressed light 312 rain frequency in STOC, the shift of rainfall intensity frequency leads to the repartitioning of ET, 313 and T/ET is increased from 51.8% to 54.3% on global land and from 57.6% to 60.7% in tropical 314 land. In addition, the dominant impact factors through which rainfall intensity affects ET and its 315 partitioning are identified through stepwise MLR analysis. It is found that solar radiation and near-316 surface dryness are important for transpiration, wet leaf fraction is important for canopy 317 evaporation in vegetated regions, and soil moisture is important for soil evaporation in desert 318 regions (Fig. 4). 319

This study focuses on the impacts of changes in rainfall frequency and associated atmospheric conditions in an atmospheric GCM due to modifications of convection parameterization on terrestrial water flux. As evapotranspiration is closely related to plant photosynthesis, the simulation of rainfall spectrum may also affect the land carbon cycle and thus the global carbon budget. For instance, photosynthesis rate may be limited through downregulation of stomatal conductance in response to increased VPD. Further research is needed in this regard, including running a fully coupled model.

327

328

320

321

322

323

324

325

326

Acknowledgments

- 329 ZC and YW are supported by the National Key Research and Development Program of China
- Grants 2017YFA0604000. GJZ is supported by the Department of Energy, Office of Science,
- Biological and Environmental Research Program (BER), under Award Number DE-SC0022064,
- and the National Science Foundation grant AGS-2054697. The TRMM 3B42 data is available
- from https://disc2.gesdisc.eosdis.nasa.gov/opendap/TRMM L3/TRMM 3B42 Daily.7/. The state of the
- GSWP-2 data is available from http://cola.gmu.edu/gswp/data.html. The FLUXCOM data is from
- 335 http://www.fluxcom.org/EF-Download/. The MSWEP data can be downloaded from
- http://www.gloh2o.org/mswep/, and the GLEAM data from https://www.gleam.eu/#downloads.
- Both are publicly available after registration. The simulation data used in this study are available
- in the open data repository Zenodo at https://zenodo.org/record/5099861.

339

340

References

- Beck, H. E., Wood, E. F., Pan, M., Fisher, C. K., Miralles, D. G., Van Dijk, A. I., et al. (2019),
- MSWEP V2 global 3-hourly 0.1 precipitation: methodology and quantitative assessment.
- Bulletin of the American Meteorological Society, 100(3), 473-500.
- Costa, M. H., Biajoli, M. C., Sanches, L., Malhado, A. C., Hutyra, L. R., Da Rocha, H. R., et al.
- 345 (2010), Atmospheric versus vegetation controls of Amazonian tropical rain forest
- evapotranspiration: Are the wet and seasonally dry rain forests any different?. Journal of
- Geophysical Research: Biogeosciences, 115(G4).
- Chen, D., Dai, A., & Hall, A. (2021). The convective-to-total precipitation ratio and the
- "drizzling" bias in climate models. Journal of Geophysical Research: Atmospheres, 126,
- e2020JD034198. https://doi. org/10.1029/2020JD034198

- De Boeck, H. J., & Verbeeck, H. (2011), Drought-associated changes in climate and their relevance for ecosystem experiments and models. Biogeosciences, 8(5), 1121-1130.
- 353 Dirmeyer, P. A., Gao, X., Zhao, M., Guo, Z., Oki, T., & Hanasaki, N. (2006), GSWP-2:
- Multimodel analysis and implications for our perception of the land surface, Bull. Am.
- 355 Meteorol. Soc., 87(10), 1381–1397, doi:10.1175/BAMS-87-10-1381.
- Gash, J. H. C., Wright, I. R., & Lloyd, C. R. (1980), Comparative estimates of interception loss from three coniferous forests in Great Britain. Journal of Hydrology, 48(1-2), 89-105.
- Good, S. P., Noone, D., & Bowen, G. (2015), Hydrologic connectivity constrains partitioning of global terrestrial water fluxes. Science, 349(6244), 175-177.
- Huffman, G. J., & Bolvin, D. T. (2013), TRMM and other data precipitation data set documentation. NASA, Greenbelt, USA, 28(2.3), 1.
- Humphrey, V., Berg, A., Ciais, P., Gentine, P., Jung, M., Reichstein, M., et al. (2021), Soil moisture—atmosphere feedback dominates land carbon uptake variability. Nature, 592(7852), 65-69.
- Jasechko, S., Sharp, Z. D., Gibson, J. J., Birks, S. J., Yi, Y., & Fawcett, P. J. (2013), Terrestrial water fluxes dominated by transpiration. Nature, 496(7445), 347-350.
- Jung, M., Reichstein, M., Schwalm, C. R., Huntingford, C., Sitch, S., Ahlström, A., et al. (2017), Compensatory water effects link yearly global land CO₂ sink changes to temperature. Nature, 541(7638), 516-520.
- Jung, M., Koirala, S., Weber, U., Ichii, K., Gans, F., Camps-Valls, G., et al. (2019), The FLUXCOM ensemble of global land-atmosphere energy fluxes. Scientific data, 6(1), 1-14.
- Laio, F., Porporato, A., Ridolfi, L., & Rodriguez-Iturbe, I. (2001), Plants in water-controlled ecosystems: active role in hydrologic processes and response to water stress: II.

 Probabilistic soil moisture dynamics. *Advances in water resources*, 24(7), 707-723.
- Li, L., Wang, Y., Arora, V. K., Eamus, D., Shi, H., Li, J., et al. (2018). Evaluating global land surface models in CMIP5: analysis of ecosystem water-and light-use efficiencies and rainfall partitioning. Journal of Climate, 31(8), 2995-3008.
- Lian, X., Piao, S., Huntingford, C., Li, Y., Zeng, Z., Wang, X., et al. (2018). Partitioning global land evapotranspiration using CMIP5 models constrained by observations. Nature Climate Change, 8(7), 640-646.
- Martens, B., Miralles, D. G., Lievens, H., Schalie, R. V. D., De Jeu, R. A., Fernández-Prieto, D., et al. (2017), GLEAM v3: Satellite-based land evaporation and root-zone soil moisture. Geoscientific Model Development, 10(5), 1903-1925.
- Massmann, A., Gentine, P., & Lin, C. (2019), When does vapor pressure deficit drive or reduce evapotranspiration? Journal of Advances in Modeling Earth Systems, 11, 3305–3320.
- Miralles, D. G., Holmes, T. R. H., De Jeu, R. A. M., Gash, J. H., Meesters, A. G. C. A., & Dolman, A. J. (2011), Global land-surface evaporation estimated from satellite-based
- observations. Hydrology and Earth System Sciences, 15(2), 453-469.

- 390 Miralles, D. G., Gash, J. H., Holmes, T. R., de Jeu, R. A., & Dolman, A. J. (2010), Global
- canopy interception from satellite observations. Journal of Geophysical Research:
- 392 Atmospheres, 115(D16).
- Mutti, P. R., da Silva, L. L., Medeiros, S. D. S., Dubreuil, V., Mendes, K. R., Marques, T. V., et
- al. (2019). Basin scale rainfall-evapotranspiration dynamics in a tropical semiarid
- environment during dry and wet years. International Journal of Applied Earth
- Observation and Geoinformation, 75, 29-43.
- Na, Y., Fu, Q., & Kodama, C. (2020), Precipitation probability and its future changes from a
- global cloud-resolving model and CMIP6 simulations. Journal of Geophysical Research:
- 399 Atmospheres, 125(5), e2019JD031926.
- Neale, R. B., Richter, J. H., & Jochum, M. (2008), The Impact of Convection on ENSO: From a Delayed Oscillator to a Series of Events. Journal of Climate, 21(22), 5904–5924.
- Neale, R. B., Chen, C. C., Gettelman, A., Lauritzen, P. H., Park, S., Williamson, D. L., et al.
- 403 (2010), Description of the NCAR community atmosphere model (CAM 5.0). NCAR
- 404 Tech. Note NCAR/TN-486+ STR, 1(1), 1-12.
- Oki, T., and Kanae, S. (2006), Global hydrological cycles and world water resources. Science, 313(5790), 1068-1072.
- Oleson, K. W., Dai, Y., Bonan, G., Bosilovich, M., Dickinson, R., Dirmeyer, P., et al. (2004),
- 408 Technical description of the community land model (CLM). Tech. Note NCAR/TN-461+
- 409 STR.
- Oleson, K. W., Lawrence, D. M., Gordon, B., Flanner, M. G., Kluzek, E., Peter, J., et al. (2010), Technical description of version 4.0 of the Community Land Model (CLM).
- 412 Peng, S., Piao, S., Ciais, P., Myneni, R. B., Chen, A., Chevallier, F., et al. (2013), Asymmetric
- effects of daytime and night-time warming on Northern Hemisphere vegetation. Nature,
- 414 501(7465), 88-92.
- Plant, R. S., & Craig, G. C. (2008), A stochastic parameterization for deep convection based on
- equilibrium statistics. Journal of the Atmospheric Sciences, 65(1), 87-105.
- Qian, T., Dai, A., Trenberth, K. E., & Oleson, K. W. (2006), Simulation of global land surface
- 418 conditions from 1948 to 2004. Part I: Forcing data and evaluations. Journal of
- 419 Hydrometeorology, 7(5), 953-975.
- Taylor, C. M., de Jeu, R. A., Guichard, F., Harris, P. P., & Dorigo, W. A. (2012), Afternoon rain
- more likely over drier soils. Nature, 489(7416), 423-426.
- Teuling, A. J., Seneviratne, S. I., Stöckli, R., Reichstein, M., Moors, E., Ciais, P., et al. (2010),
- 423 Contrasting response of European forest and grassland energy exchange to heatwaves.
- 424 Nature geoscience, 3(10), 722-727.
- Trenberth, K. E., Dai, A., Rasmussen, R. M., & Parsons, D. B. (2003), The changing character of
- precipitation. Bulletin of the American Meteorological Society, 84(9), 1205-1218.
- Wang, K., & Dickinson, R. E. (2012), A review of global terrestrial evapotranspiration:
- Observation, modeling, climatology, and climatic variability. Reviews of
- 429 Geophysics, 50(2).

430 431 432	Wang, Y., & Zhang, G. J. (2016). Global climate impacts of stochastic deep convection parameterization in the NCAR CAM 5. Journal of Advances in Modeling Earth Systems 8(4), 1641-1656.
433 434 435	Wang, Y., G. J. Zhang, and G. C. Craig (2016), Stochastic convective parameterization improving the simulation of tropical precipitation variability in the NCAR CAM5, Geophys. Res. Lett., 43, doi:10.1002/2016GL069818.
436 437 438 439	Wang, Y., Zhang, G. J., Xie, S., Lin, W., Craig, G. C., Tang, Q., & Ma, H. Y. (2021), Effects of coupling a stochastic convective parameterization with the Zhang–McFarlane scheme or precipitation simulation in the DOE E3SMv1. 0 atmosphere model. Geoscientific Model Development, 14(3), 1575-1593.
440 441 442	Wei, Z., Yoshimura, K., Wang, L., Miralles, D. G., Jasechko, S., & Lee, X. (2017), Revisiting the contribution of transpiration to global terrestrial evapotranspiration. Geophysical Research Letters, 44(6), 2792-2801.
443 444 445 446	Zhang, G. J., and McFarlane, N. A. (1995), Sensitivity of climate simulations to the parameterization of cumulus convection in the Canadian Climate Centre general circulation model. Atmosphere-ocean, 33(3), 407-446.

447	References From the Supporting Information
448 449 450	Park, S., & Bretherton, C. S. (2009), The University of Washington Shallow Convection and Moist Turbulence Schemes and Their Impact on Climate Simulations with the Community Atmosphere Model. Journal of Climate, 22(12), 3449-3469.
451 452	Bretherton, C. S., & Park, S. (2009), A New Moist Turbulence Parameterization in the Community Atmosphere Model. Journal of Climate, 22(12), 3422-3448.
453 454 455	Iacono, M. J., Delamere, J. S., Mlawer, E. J., Shephard, M. W., Clough, S. A., & Collins, W. D. (2008), Radiative forcing by long-lived greenhouse gases: Calculations with the AER radiative transfer models. Journal of Geophysical Research, 113(D13), D13103.
456 457 458 459	Lawrence, D. M., Thornton, P. E., Oleson, K. W., & Bonan, G. B. (2007). The partitioning of evapotranspiration into transpiration, soil evaporation, and canopy evaporation in a GCM: Impacts on land–atmosphere interaction. Journal of Hydrometeorology, 8(4), 862-880.
460 461	Morrison, H., & Gettelman, A. (2008), A New Two-Moment Bulk Stratiform Cloud Microphysics Scheme in the Community Atmosphere Model, Version 3 (CAM3). Part I:
462 463	Description and Numerical Tests. Journal of Climate, 21(15), 3642–3659. https://doi.org/10.1175/2008JCLI2105.1